ECRH at W7-AS

V. Erckmann [1] , H.P. Laqua [1], H. Maaßberg [1], N. B. Marushchenko [1], M. Rome'[2], F. Volpe [1], W. Kasparek [3], G.A. Müller [3], W7-AS Team [1]

[1] Max-Planck-Institut für Plasmaphysik, EURATOM Ass., Teilinstitut Greifswald, D-17491 Greifswald, Germany
[2] Dipartimento di Fisica, Universita' degli Studi di Milano, Milano, Italy
[3] Institut für Plasmaforschung, Universität Stuttgart, D-70569 Stuttgart, Germany

E-mail: volker.erckmann@ipp.mpg.de

Abstract: ECRH started 20 years ago at IPP using 28 GHz (200 kW) at the W7-A stellarator. The physics achievements were strongly linked to the progress in source and transmission/launching technology. The capability and versatility of ECRH is reviewed using W7-AS, which was shut down in July 31, 2002, as an example experiment. The ECRH-experiments cover a plasma parameter range with electron temperatures of up to 6.8 keV and densities up to 3.5×10^{20} m^{-3}. Milestone achievements are discussed. Standard heating scenarios such as O-mode, X-Mode as well as mode-conversion heating via the O-X-B process at different harmonics were investigated and selected results are presented. The physics of wave interaction with stellarator specific trapped particle populations is dicussed. First experiments with current drive by Bernstein-waves are reported.

1 Introduction

The operation of the W7-AS stellarator was terminated on Juli 31, 2002 and the experimental stellarator research at IPP is now focussed on the construction and operation of the W7-X stellarator. The ECRH-activities started 20 years ago at W7-A [1]. The progress in ECRH was closely linked to the technological development of sources operating at higher frequency (to match the resonance condition for higher magnetic induction), and higher microwave power (to achieve fusion relevant plasma parameters). The 28 GHz system at W7-A was replaced one year later by a 70 GHz system, and the first flexible in-vessel launcher with steerable launching mirrors was invented by the IPF-Stuttgart group [2] and installed in W7-AS in Oct. 1988. This key technology allowed a detailed investigation of phase-space wave-particle interaction physics in a wide range from perpendicular (ECRH) to oblique launch (ECCD) at on- and off-axis deposition. Some example experiments on power deposition and current drive together with the theoretical modeling are presented in Section 2 and 4. W7-AS saw then the upgrading of ECRH to 1 MW microwave power at 70 GHz (5 Gyrotrons, 200 kW each, 3 s). The frequency related density restrictions, however, remained, while the stellarator confinement did not show a density limit. The first 140 GHz, 0.8 MW, 0.5 s gyrotron was provided by the russian institute IAP Nizhny Novgorod thus shifting the density operation regime towards 1.2×10^{20} m^{-3} . The system became operational for W7-AS in 1993 marking a milestone in ECRH technology [3]. An upgrade followed resulting in a two frequency-installation with 2.3 MW at 140 GHz and 0,5 MW at 70 GHz. The latter was maintained to keep the option of 1.25 T operation open. The high available ECRH-power led to the discovery of new confinement regimes such as H-mode [4] and 'electron-root' confinement. Selected experiments are discussed in Sec. 3. The experiments in the last period of the W7-AS lifetime were focussing on the ß-limit and island-divertor operation. Both require high density operation. Efficient Bernstein-wave heating via the O-X-B mode conversion process overcomes the density limitations [5] and experiments up to 3.5×10^{20} m^{-3} are discussed in Sec. 5. Here O, X, and B are the ordinary, extraordinary and Electron-Bernstein-Mode. Instead of an upper density limit, as for the standard ECRH-scenarios, a lower density limit exists for this scenario at $n_{e,crit} = 2.5 \times 10^{20}$ m^{-3} for 2nd harmonic at 140 GHz. Current drive results with Bernstein waves in high density plasmas are discussed in the light of Fokker-Planck calculations.

2 Power deposition

On-and off axis heating was shown already at W7-A [6] by tuning the magnetic field and thus the resonance layer. The improved launcher at W7-AS with in-vessel launching mirrors [2] allowed to steer each microwave beam to arbitrary poloidal and toroidal launch angles. An example for off-axis heating with two microwave beams of 0.2 MW each in X2 mode (B_o = 1.25 T) and resonance on-axis is shown in Fig.1 together with the ray tracing calculations in the 3-D stellarator geometry. The profiles of n_e and T_e for off-axis heating are compared to on-axis heating. Whereas the T_e-profile changes from peaked (on-axis deposition) to hollow (off-axis deposition), the n_e-profile shows only a small change from slightly hollow (on-axis) to flat (off-axis). The discusssion of the density profile effect is beyond the scope of this paper.

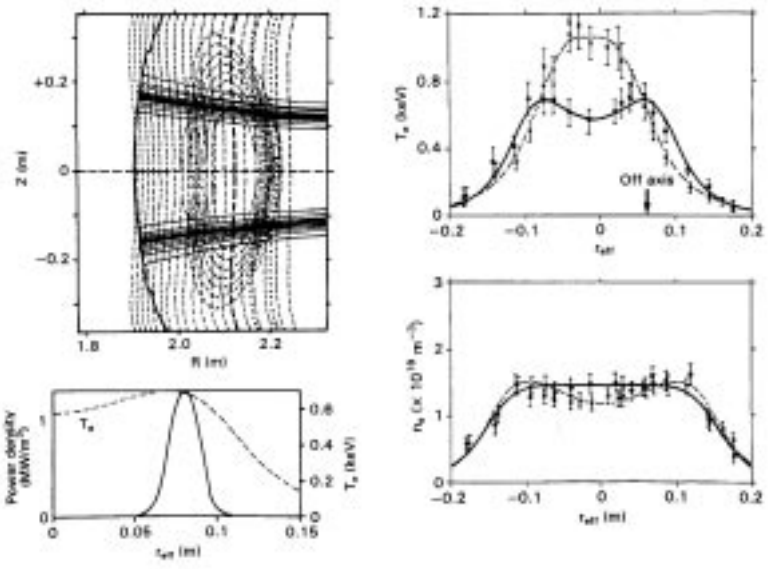

FIG. 1: *Ray tracing calculations for off-axis heating with two rf-beams at W7-AS (left) and related profiles of the electron temperature T_e and density n_e (right). W7-AS flux-surfaces are shown together with contours of /B/=const. (almost vertical dashed lines with the resonance layer on axis) and the microwave rays (top, left). The off-axis power deposition profile is shown on left, bottom. The n_e (right, bottom) and Te- profiles (right, top) for off-axis heating (solid line) are compared to on-axis heating (dashed line).*

The narrow power deposition of ECRH can be used to stimulate a localized periodic perturbation of the electron temperature by ECRH power modulation. This perturbation propagates outward from the deposition region in the plasma thus driving a heat wave. From the local measurement of the phase and amplitude of this heat wave both, the heat transport coefficient of the plasma and the power deposition profile can be determined locally [7,8]. In the experiment described here the deposition profile was derived from the analysis of stimulated heat waves in ECRH power modulation experiments, with the time dependent electron temperatures from ECE measurements (see Fig. 2). The ECRH-power was modulated with an amplitude of 10 - 30 % and different frequencies from 0.05 - 5 kHz. This kind of analysis requires a proper modelling of the transport effects in the transient energy balance. The heat transport was described by a purely diffusive model. No evidence for a significant convective contribution was found. Peaked deposition profiles are usually obtained for both O- and X-mode heating from a 3D Hamiltonian ray-tracing code based on the assumption of a Maxwellian electron distribution function (single pass absorption). From the heat transport analysis of modulation experiments we obtain similarly peaked absorption profiles, but additionally a much broader contribution is present (see Fig. 2), whose width and relative integral contribution with respect to the "thermal" peaked part depends on the particular heating scenario, magnetic configuration and collisionality regime. The measured broadening

of the deposition profile is attributed to the fast transport via the drift orbits of trapped electrons in the long mean free path regime [8]. Taking the broader component of the power deposition profile into account, the input power is recovered by the heat transport analysis within the errors.

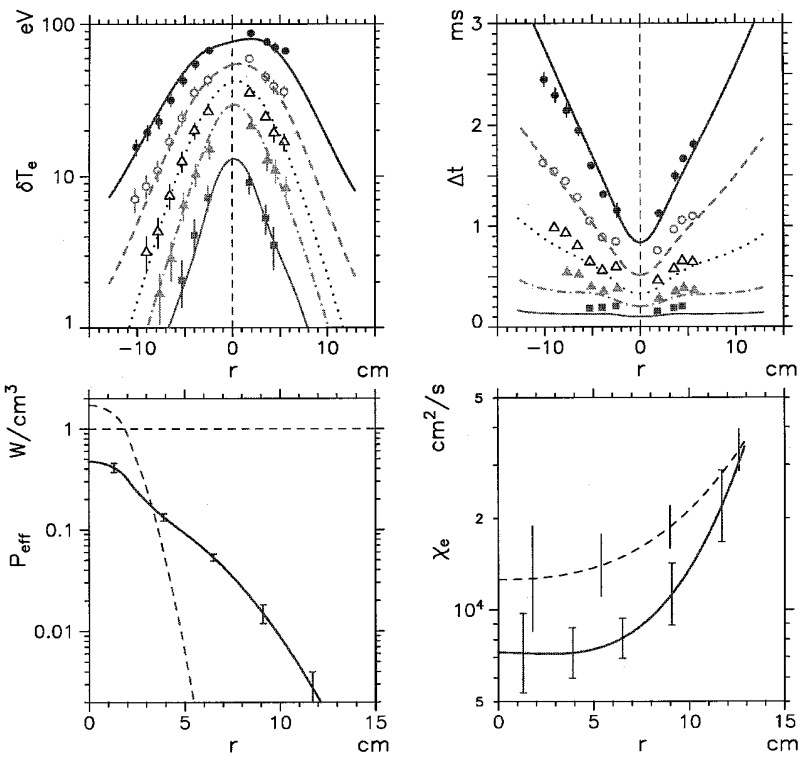

FIG. 2: *The temperature modulation amplitudes δTe and the time delays, Δt, versus radius, r, for different modulation frequencies, f_{mod} = 92, 200, 400, 800 and 2000 Hz (upper left and right plots) from ECRH power modulation experiments at B_0 = 2.5 T (O1-mode, 70 GHz) with on-axis deposition. The power deposition profile (lower left, solid line) is compared to the "ray-tracing profile" shape (dashed line). The plot on the right gives the "effective" heat conductivity, $\chi_e(r)$ (solid line). For comparison, the $\chi_e(r)$ profile from the stationary power balance analysis is also shown (dashed line).*

3 Improved confinement: The 'electron root'

Experiments with strong X2-mode heating from the low field side in the equatorial plane were performed in a wide density and power range. The central electron temperatures range from 5.7 keV at 1.7 x 10^{19} m^{-3} to 3 keV at 7.5 x 10^{19} m^{-3} at constant input power of 1.2 MW. A pronounced steepening of the temperature gradients is seen in the centre of the plasma [9] at densities below 4 x 10^{19} m^{-3}. A similar behaviour was measured during a power scan at constant density of 0.2 x 10^{20} m^{-3}, where the steepening occurred between 0.2 and 0.4 MW. Radial profiles of T_e and n_e are shown in Fig. 3 for discharges with different heating power at constant density. The stationary transport analysis of these discharges results in a central (r/a < 0.3) electron heat diffusivity, which is well below the neoclassical heat diffusivity, once electric fields are neglected. Strongly positive radial electric fields up to 50 kV/m were measured in the plasma center, which lead to good agreement with neoclassical theory including electric fields ('electron root solution'). It is worth noting, that the ions are energetically decoupled from the electrons under these conditions and the energy balance is dominated by the electrons. The appearance of the electric fields and the corresponding steep temperature gradients shows a threshold at a density around 0.2 - 0.4 x 10^{20} m^{-3} for a heating power of 1.2 MW and a power threshold around 02 - 0.4 MW for constant density of 0.2 x 10^{20} m^{-3} (see Fig. 3). The discharge could be placed at the threshold by careful adjustment of the heating power density while tuning the deposition region.

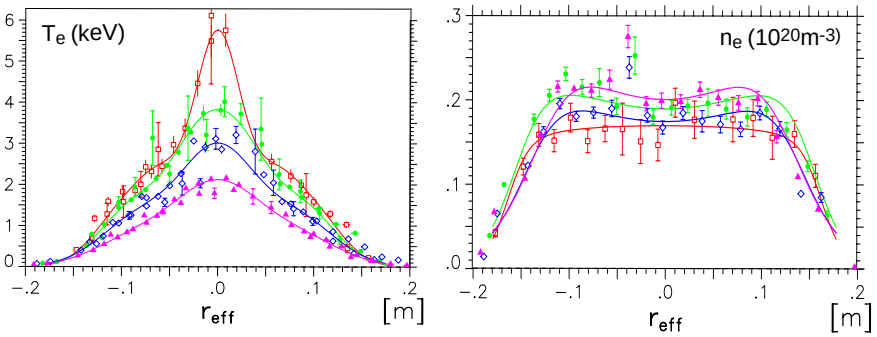

FIG. 3: *Radial profiles of the electron temperature (left) and density (right) at different heating power of 0.2 (triangles), 0.4 (open circles), 0.8 (dots) and 1.2 MW (squares).*

The central electron temperature then is jumping between two states of low (say 4 keV) and high (5 keV) temperature during one discharge with some hysteresis between rise and fall-time constants. The experiments are explained by a substantial loss of fast trapped particles driven by ECRH itself, which in turn generates a positive electric field with its beneficial effect on the bulk electrons. This picture is consistent with the results of switching experiments, where the central confinement is lost on a fast timescale (< 0.3 ms), whereas the remaining profile relaxes on the diffusion timescale.

4 Electron Cyclotron Current Drive

Stellarators are well suited for the investigation of ECCD, because the sensitivity limitations for the measurement of small currents are much lower as compared to tokamaks, where the EC-driven currents have to be discriminated against large inductively driven currents. Furthermore, the flexibility in the magnetic configuration allows to investigate the current drive physics and the related wave particle interaction in phase space with high accuracy.

The EC-wave absorption increases the perpendicular energy of electrons and thus particles, which are trapped in magnetic mirror fields have significant influence on the CD-efficiency. Current drive modeling [10] tends to overestimate the CD-efficiency by a factor of 2-3 if trapped particle effects are neglected. The role of trapped particles in the ECCD physics was investigated by operating W7-AS in different magnetic mirror configurations. A launch angle scan was performed with inductive compensation of the EC driven current (I_p=0) for two magnetic configurations with a similar toroidal magnetic mirror ratio as shown in Fig.4. The fraction of trapped particles, however, was changed by changing the toroidal ripple on the magnetic axis in the toroidal position of power launching at φ = 36 °. For case 1 the magnetic mirror maximum was placed in the ECRH plane, i.e. mainly passing particles are directly heated and the impact on the driven current is mainly by the friction with the background trapped particles (dotted line in Fig. 4). For case 2 the minimum of the magnetic mirror was placed in the ECRH plane and, following ray tracing predictions the power is mainly absorbed by trapped and barely passing particles (dashed line in Fig. 4). As seen from Fig. 5, the loop voltage at perpendicular launch (φ =0) with no ECCD is non-zero for both cases and represents the voltage for bootstrap current compensation. The loop voltage and thus the driven current is much larger in case 1 (Fig. 5, top, left, note the different scales) as compared to case 2 (Fig. 5, top, right). A large fraction of ECCD power is absorbed in this case directly by trapped particles, which do not contribute to current drive. The ECCD efficiency even changes sign in case 2, which is a consequence of the ECRH induced trapping of otherwise barely passing particles. The experimental results agree well with the CD-efficiency from linear theory (Fig. 5, (bottom)) [11].

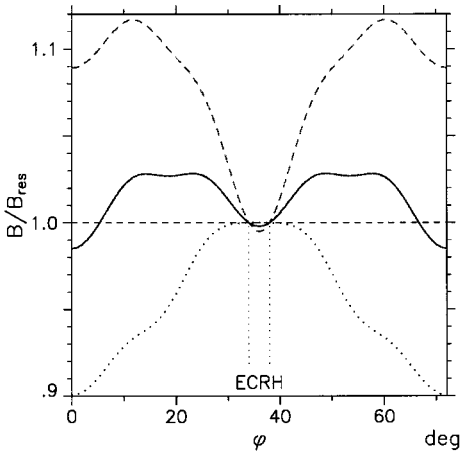

FIG. 4: *Magnetic field strength on-axis, normalized to the resonant field at the ECRH launching position, versus the toroidal angle within one field period for* $i_a \sim 0.345$*. The solid line refers to the "standard" configuration of W7-AS, the dashed and the dotted lines correspond to the "minimum B" and the "maximum B" launching scenarios, respectively.*

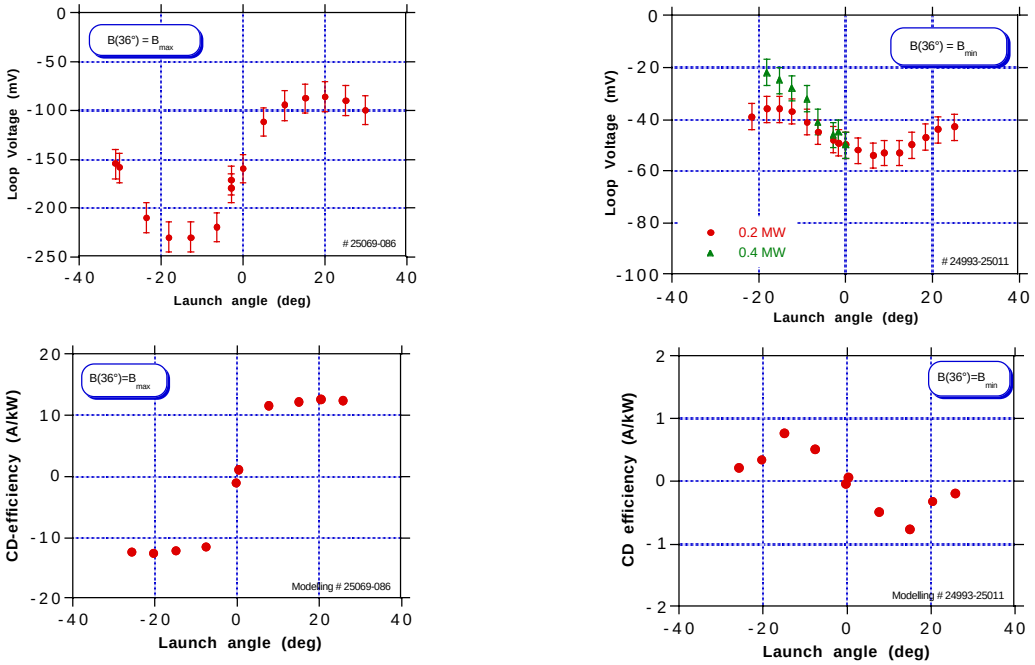

FIG. 5: *Effect of trapped particles on ECCD. Top**:** Loop voltage response on a launch angle scan with plasma net current Ip=0 for two magnetic field configurations in W7-AS. The ECCD power is 0.4 (triangles) and 0.2 MW (dots). Bottom**:** Current drive efficiency from linear theoretical modelling.*

5 Mode conversion heating and current drive via the O-X-B Process

The standard ECRH scenarios have intrinsic density limitations by the cut-off condition. In view of reactor relevant conditions it may be desirable to have ECRH-access to even higher densities. This is provided by O2-mode launch, which is a promising candidate at W7-X [12]. The O-X-B mode conversion process [13] is another scheme to overcome density limitations. The essential part of this scheme is the conversion of an O-wave at oblique launch from the

low field side into an X-wave at the O-wave cut-off layer [14]. The X-wave then propagates back to the upper hybrid resonance layer where the conversion into EBWs takes place. The EBWs propagate towards the plasma centre where they are absorbed by electron cyclotron damping. Efficient OXB-heating with 70 GHz 1st harmonic EBWs was successfully demonstrated at W7-AS [5] but the higher harmonic O-X-B heating with 140 GHz EBWs remained unexplored until improved performance by divertor operation above the critical density of 2.4 10^{20} m^{-3} was achieved recently. Three 140 GHz beams with a total power of 1.5 MW were launched into an NBI sustained (up to 4 MW) high-density plasma (up to 3.5 10^{20} m^{-3}). Here the optimisation criterion was the increase of plasma energy as shown in Fig.6 (left) during the heating pulse and the related reduction of the non-absorbed ECRH stray radiation. A magnetic field scan was performed to achieve power deposition near the plasma center. The power deposition was estimated from heat wave modulation experiments as described in Sec. 2 using Electron Bernstein wave Emission (EBE) diagnostic for the electron temperature measurement [15]. The result for 2nd harmonic (B2) is shown in Fig. 6 (right) with power deposition at r/a = 0.3. The apparent asymmetry of the power deposition is due to the strong shafranov-shift of the plasma, which could not be taken into aaccount completely in the EBE temperature-profile reconstruction. The central plasma temperature rises from about 270 eV to 310 eV during the EBW-heating and the temperature profile broadens. The total stored plasma energy increases during EBW-heating by about 40% and about half of this energy increase is due to the profile change. Since the plasma is optically thick for higher harmonic EBW, also third and fourth harmonic heating was successfully demonstrated with 140 GHz at 1.5 T and 1.1 T, respectively.

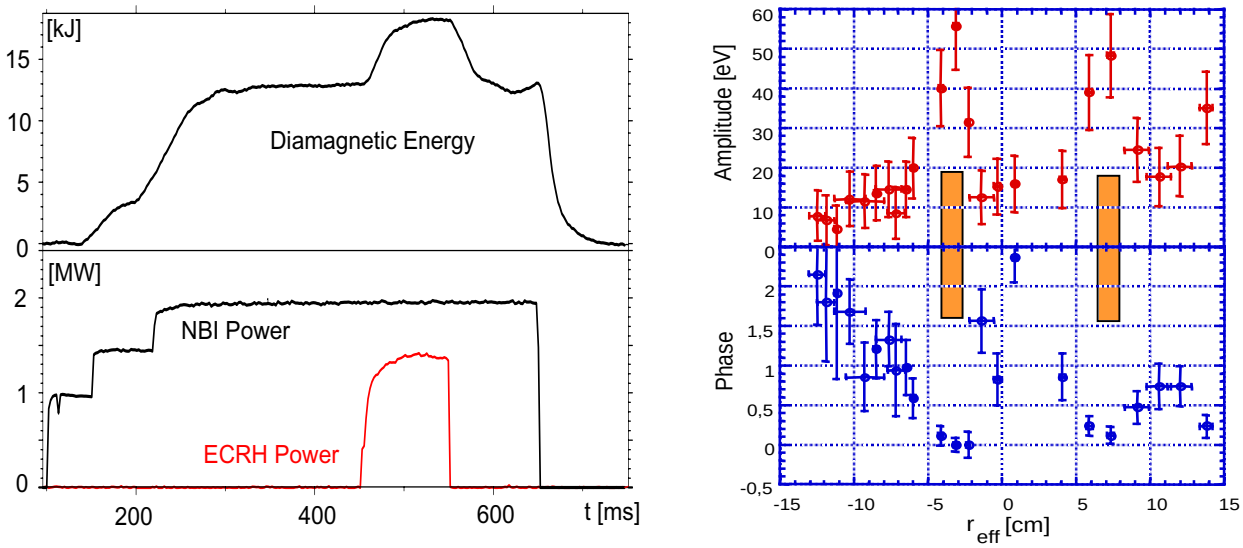

***Fig.6**: **left:** Total stored plasma energy (top) and heating power(bottom) as a function of time during Electron Bernstein-Wave heating with 140 GHz) at a density of 3.5 10^{20} m^{-3} and B_o = 2.12 T.*
Right: *Heat wave amplitude and phase from 2nd harmonic (140 GHz) modulated O-X-B-heating for a similar discharge. The data are reconstructed from first harmonic EBE-diagnostic.*

Recently we have performed CD-experiments with EB-waves. Due to their electrostatic character the parallel component of the refractive index can become of the order of 1 implying a high EBW current drive (EBCD) efficiency [15]. Since the CD efficiency scales like T_e/n_e the experiment were performed with 0.45 MW at 70 GHz first harmonic EBW-heating at a density of 1.05 10^{20} m^{-3}. The magnetic field was adjusted to 2.15 T for central power deposition. Here the large $N_{||}(\approx 1)$ component of the EBWs requires a stronger reduction of the resonant magnetic field than for standard ECCD with electromagnetic waves. Since O-X-B mode conversion requires a fixed optimal launch angle no angular scan is possible to investigate the driven current. However the $N_{||}$ component of the EBWs was varied by both, the magnetic field reversal and the change of the magnetic configuration, (see Fig. 4).

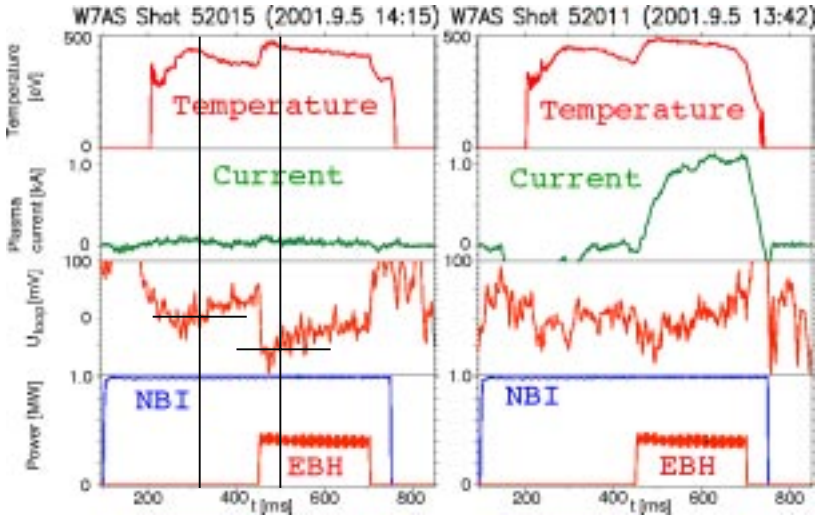

FIG. 7: *EBW-Current Drive at a plasma density of 1.1 10 ^{20} m^{-3}. Net current free discharge with inductive compensation of the EBCD current (left) and with free running plasma current (right).*

The loop voltage represents a measure for the driven current in net current free discharges. The highest CD efficiency (see Fig 7) was achieved in the case of co-EBCD Here with 450 kW a driven current of 1.85 (+1,-0.5) kA was derived from the measured data. In a similar discharge, but with zero loop voltage, the plasma current rises to about 1.2 kA during the EBW-CD. Fokker-Planck calculations were performed for the experimental plasma parameters to estimate the distortion of the electron distribution function and the resulting current. Due to a large $N_{||}$ value and to the associated strong Doppler shift, the EC-interaction takes place at more than two times the thermal velocity. Thus the quasi-linear diffusion is situated well outside the trapped electron loss cone, as illustrated in Fig.8. The resonance curve is no longer an ellipse as for $|N_{||}|<1$, but become a parabola for $|N_{||}|=1$ and a hyperbola for $|N_{||}|>1$. The perpendicular refractive index $N_{\perp}$ is about 40, which means that the wave length is of the order of the gyro radius. In that case the quasi-linear diffusion operator splits into many maxima (see Fig.8). The calculated current is in agreement with the experimental results within the error bars.

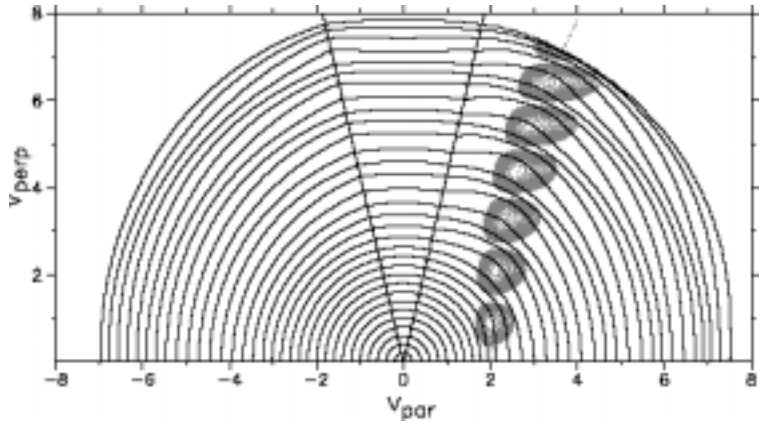

FIG. 8: *Contours of the electron distribution function. The parallel, $V_{par,}$ and the perpendicular velocity, $V_{perp,}$ are normalised to the thermal velocity. The grey structure is the quasi-linear diffusion operator for EBWs with $N_{||}$ =1.0. The calculation was limited to $|V|<8V_{thermal}$.*

6 Conclusions

ECRH and ECCD was investigated in the IPP Stellarators W7-A and W7-AS. Significant contributions to the physics understanding of the wave-particle interaction in complex stellarator magnetic configurations were made. The deposition profiles in the long mean free path regime are affected by the wave interaction with trapped particles. The measured profiles consist of a narrow peaked component, which contains the main power fraction (70 - 100 %) and a second component, which contains up to 30 % of the total power and is much broader. This part depends on the number and distribution of trapped particles. The direct and indirect (friction of passing particles with background trapped electrons) interaction of trapped particles with EC-waves affects the current drive efficiency as measured in experiments with different magnetic mirror configurations and verified by CD-theory. Improved confinement modes were discovered which are related to strong ECRH. The rapid loss of trapped particles, which are pushed into the loss-cone by ECRH generates strong positive electric fields (‘electron root’) in the plasma centre, which in turn improves the central bulk confinement. Mode conversion heating and current drive via the O-X-B process extends the ECRH application towards high densities beyond the cut-off density of the O-mode. Efficient O-X-B heating was demonstrated for the first time up to the fourth harmonic resonance at W7-AS. The efficiency of the process is determined by the density gradient scale length as well as density fluctuations at the O-X-conversion layer. First EBW current drive experiments in overdense plamas were investigated and good agreement with Fokker-Planck modeling is obtained.

References

[1] Wilhelm, R., Janzen, G., Müller, G., et al., Plasma Phys. and Contolled Fusion 26, (1984) 259

[2] Erckmann, V., W7-AS Team, W. Kasparek, et al., Fusion Technology, Vol. **17**, (1990), p. 76

[3] Erckmann, V., N. Alexandrov, V.I. Il'in, V.I. Kurbatov, et al. Proc. 20th EPS Conf. Contr. Fusion and Plasma Physics, Lisboa, Portugal, Vol **17C**, (1993) 345

[4] Erckmann, V., S.D. Bogdanov, A.A. Borschegovsky, et al. Phys. Rev. Lett. **70**, 14, (1993) 2086

[5] H. P. Laqua, V. Erckmann, H.J. Hartfuß, H. Laqua, W7-AS Team, and ECRH Group, Phys. Rev. Lett. **78**, 3467 (1997)

[6] Erckmann, V., W7-A Team, NI-Team (W7-A5) and ECRH Group (IPF Stuttgart), Plasma Physics and Controlled Fusion **28**, 9A, (1986), p. 1277

[7] Hartfuß, H.J., H. Maaßberg, M. Tutter, W7-A Team, ECRH Group, Nuclear Fusion 26, (1986), p. 678

[8] U. Gasparino, V. Erckmann , H.J. Hartfuß, H. Maaßberg, M. Rome’, Plasma Phys. Control. Fusion **40** (1998) 233-244

[9] H. Maaßberg, C.D. Beidler, V. Erckmann, U. Gasparino, J. Geiger, H. Laqua, N. Marushchenko, S. Murakami and the W7-AS Team, Strong Microwaves in Plasmas, Editor A.G. Litvak, Inst. of. Appl. Physics, Nizhny Novgorod, Russia, Vol.1 (2000) p. 7-26

[10] Gasparino, U., Theory of Fusion Plasmas, Varenna, (1990) 195

[11] U. Gasparino, H. Idei, S. Kubo, N. Marushchenko, M. Rome‘, Nucl. Fusion 38, No.2, (1998) 223

[12] Erckmann, V., Karulin, N. and Wobig, H., Proc. 21st EPS Conference on Controlled Fusion and Plasma Physics, Vol 18B, Part II, (1994), p. 1008

[13] J. Preinhaelter and V. Kopecky, J. Plasma Phys. 10 (1973) 1;

[14] E.Mjølhus, J. Plasma Phys. 31 (1984) 7;

[15] F.Volpe and Laqua, accepted for publication in Rev. Sci. Instrum. 74. Issue1 (Jan. 2003)

[16] A.G. Litvak et al., Phys. Letters A. 188, 64 (1994)